Hindawi
Advances in Civil Engineering
Volume 2021, Article ID 5580555, 19 pages
https://doi.org/10.1155/2021/5580555

Research Article

Experimental Study on Anchorage Performance of Resin Grout with Steel Segment

Junchao Shen [1,2]

[1]*School of Energy Science and Engineering, Henan Polytechnic University, Jiaozuo 454000, China*
[2]*Changzhi Vacational and Technology College, Changzhi 046000, China*

Correspondence should be addressed to Junchao Shen; alaskaboy@126.com

Received 14 January 2021; Revised 19 March 2021; Accepted 3 May 2021; Published 26 May 2021

Academic Editor: Wayne Yu Wang

With the advantages of large anchoring force and fast anchoring speed, resin cartridge has become the main anchoring means of geotechnical engineering and underground space engineering support. Based on the theoretical analysis, it is clear that adding aggregate can improve the mechanical properties of grout and the bolt-grout interface stress state; the mechanical properties of aggregate are positively correlated with its improvement effect on anchorage performance. By using the numerical simulation method, it is concluded that the addition of steel segments into the resin grout can improve the stiffness of the anchorage system and enhance the energy absorption and antifailure ability of the anchorage system. Relying on the self-developed anchorage mixing device, the effects of steel segment diameter and addition amount on the anchoring force were studied experimentally, and the optimal addition amount of different types of steel segment to improve the maximum anchoring force was determined.

1. Introduction

Anchor support is a kind of reinforcement technology widely used in geotechnical engineering, which could significantly improve the stability of supporting objects, so it is recognized as an effective supporting method. For the bolt support system, Windsor proposed the concept of bolt load transfer mechanism [1]. The system consists of four parts: rock, external fixtures, internal fixtures, and reinforcement elements. Reinforcement and external fixtures include bolts, plates, and nuts. Rock and reinforcement elements are coupled with bolt-rock friction or grout, which include cement or polymer resin.

The bond strength between grout and bolt is an important factor to determine the bearing capacity of the anchorage system [2, 3]. Decoupling often occurs along with the bolt-resin interface, which will lead to the failure of the anchorage system. Some researchers have studied the bond mechanism between bolt and grout and pointed out that the bearing capacity of the bolt-resin interface consists of three forms: adhesion, interlock mechanism, and friction [4, 5]. For the internal fixtures, resin cartridges have been widely used owing to their high bonding strength, rapid curing, and high safety and reliability. The resin cartridge is composed of polymer resin, high strength filler, catalyst, and other auxiliary materials, whose the working principle is to use separate packages to completely isolate the resin and the catalyst [6]. When used in the support process, resin cartridges are pushed into the hole with the bolt; then the bolt is rotated to mix the resin by the drilling rig. The curing reaction takes place when the two substances are fully mixed, hence bonding the bolt to the surrounding rock. Figure 1 shows the process of bolt installation and mixing.

Many scholars have made fruitful research on the influencing factors of anchoring force to improve the bearing capacity of the anchorage system. Hu et al. performed the pullout test of resin bolt at different temperatures. The results show that the temperature has a great influence on the anchorage performance; the anchoring force of resin grout reaches its peak value when the temperature is at 25°C, and the increase or decrease of temperature will affect the anchoring force [7]. Aziz et al. carried out a series of pullout tests and found that mixing time and bolt hole parameters have a significant impact on the

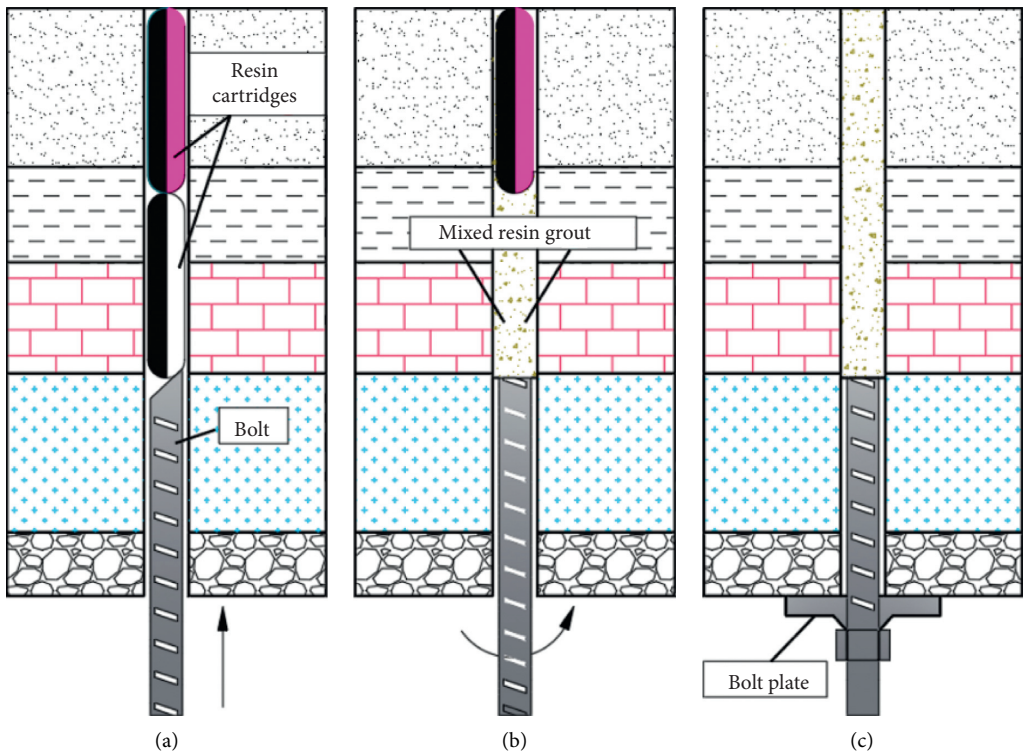

Figure 1: Bolt installation process. (a) Resin cartridges are inserted into the hole and pushed to the top of the bolt hole with the bolt. (b) Bolt is then rotated to mix the resin. (c) Rotation is stopped, followed by thrusting the bolt plate against the roof surface.

anchoring force; approximately 10 s constitutes a suitable time for bolt installation; and the drilling of bolt holes contributes to improving load transfer capacity [8]. Skrzypkowski et al. tested the flexibility and load-bearing capacity of the Olkusz-16A bolt, which was equipped with a steel coil; the laboratory test results indicated that the installing depths of 0.2 m and 0.028 m diameter bolt hole have the higher bearing capacity [9]. According to the test results, Zhang et al. and He et al. found that the amount of water inflow had a certain influence on the anchoring force of the resin bolt, and with the increase of water inflow, the anchoring force decreases [10, 11]. Kang et al. considered that the strength of surrounding rock had an obvious influence on anchoring force. Under the same anchoring force, the anchorage length of soft rock should be greater than that of hard surrounding rock [12]. Skrzypkowski et al. researched the deformation energy of flat and profiled dome bearing plates and found that the amount of energy absorbed of bolt equipped with dome bearing plate has 2.6 times than the flat one. The higher the height of the dome, the higher the energy absorption [13].

Concrete has been widely used in the field of civil engineering. The addition of aggregate to concrete has been found to improve the shear strength, compressive strength, and tensile strength, and the results show that reasonable aggregate and mixing ratio can effectively improve the mechanical properties of concrete members [14–16]. Based on these experimental results, by adding aggregate to resin grout to improve the anchoring force, as illustrated in Figure 2, the influence of external uncertain factors can be

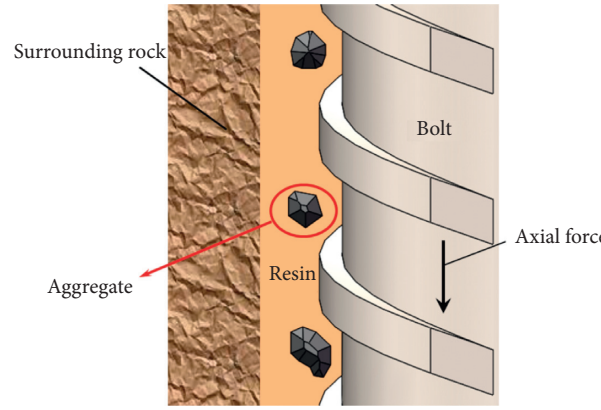

Figure 2: Schematic diagram of adding aggregate into resin grout.

effectively avoided. However, there are still a few more research works in this field. You and Zhan proposed the mortar under certain strength conditions; the higher the sand content of the grout, the greater the anchoring force. The analysis shows that the deformation of grout interface with high sand content will produce more volume expansion. Due to the constraint of the matrix material, a higher confining pressure is generated; as a result, the anchoring force increases [17]. Cao et al. and Zhang et al. studied the change of anchoring force after adding metal particles to resin; the pullout test results showed a certain effect on the improvement of anchoring force [18–20]. However, the above research works only stay in the experimental stage; the

mechanical working mechanism and mechanical properties of additives in the anchorage system were not elaborately proposed.

In this paper, the mechanical mechanism of the interface between the bolt and resin grout with aggregate was studied using theoretical analysis. Based on this, it is concluded that the mechanical parameters of resin grout can be further improved by adding steel segments, thereby improving the anchorage performance. By using the finite element numerical simulation software ABAQUS, we presented a numerical modeling that could be applied for evaluating the working performance of resin grout with steel segment, the displacements, axial load, and stress of bolt and resin grout could be obtained. Finally, through the laboratory experiment, the change law of the bearing capacity of the anchorage system under the conditions of different steel segment adding amount and length diameter ratio was analyzed, and the optimal adding amount and length diameter ratio were determined. The research results can provide a new idea for improving the anchorage effect of rock bolt support in geotechnical engineering.

2. Working Mechanism of Resin Grout with Steel Segment

2.1. Analysis of the Interface Mechanical Effect of Bolt-Grout after Aggregate Mixed into Resin. The mechanical properties of resin grout can be improved by adding aggregate. In order to study the relationship between the resin grout properties and load transfer, the shape of the bolt was simplified, so the rib was neglected. Moreover, it is assumed that the relative slip occurs at the bolt-grout interface, so as to exclude the influence of surrounding rock mechanical properties on anchoring force.

The Mindlin displacement solution is used to calculate the stress distribution of resin grout. The established analysis model is shown in Figure 3(a). According to the Mindlin solution, a concentrated force P is applied at the depth h from the surface. The induced vertical displacement at any point $A(x, y, z)$ is $w(z)$ [21]:

$$w(z) = \frac{P}{16\pi G(1-\mu)}\left[\left(\frac{(3-4\mu)}{R_1}\right)+\left(\frac{8(1-\mu)^2-(3-4\mu)}{R_2}\right)+\left(\frac{(z-h)^2}{R_1^3}\right)+\left(\frac{(3-4\mu)(z+h)^2-2zh}{R_2^3}\right)+\left(\frac{6zh(z+h)^2}{R_2^5}\right)\right], \tag{1}$$

$$R_1 = \sqrt{\left(x^2+y^2\right)+(z-h)^2},$$
$$R_2 = \sqrt{\left(x^2+y^2\right)+(z+h)^2}, \tag{2}$$

$$G = \frac{E}{2(1+\mu)}. \tag{3}$$

As shown in Figure 3(b), for the convenience of analysis, the initial anchorage section is regarded as $O(0, 0, 0)$, where the concentrated force is P. Assuming that the axial force on the grout is $P(z)$ in the z-axis direction, the vertical displacement of point $B(0, 0, z)$ caused by $P(z)$ can be simplified as

$$w(z) = \frac{P(z)(3-2\mu)}{4\pi G z}. \tag{4}$$

Substituting equation (3) into equation (4) yields

$$w(z) = \frac{P(z)(1+\mu)(3-2\mu)}{2\pi E z}. \tag{5}$$

The microelement of the bolt in Figure 3(c) is taken for analysis, and its length is dz. The z-direction equilibrium equation is written as follows:

$$\mathrm{d}P(z) = \pi \mathrm{d}\tau(z)\mathrm{d}z. \tag{6}$$

If the anchorage length is l, the total displacement at the bottom of resin grout is

$$w = \int_0^l \frac{(3-2\mu)(1+\mu)}{2E}\frac{\mathrm{d}\tau(z)}{z}\mathrm{d}z, \tag{7}$$

where E is the elastic modulus of resin grout with aggregate and μ is Poisson's ratio of resin grout with aggregate.

The axial force distributed along the bolt is

$$P(z) = -\int_0^l \pi \mathrm{d}\tau(z)\mathrm{d}z, \tag{8}$$

where d is the diameter of the bolt.

The total elongation of the bolt at the bottom of the grout is given by

$$w_b = -\int_0^l \frac{1}{E_b A}\left(\pi\, d\int_0^l \tau(z)\mathrm{d}z\right)\mathrm{d}z, \tag{9}$$

where E_b is the elastic modulus of the bolt and A is the cross-sectional area of the bolt.

In the elastic stage, there is no relative slip between the bolt and the grout, the same deformation of bolt and grout at this stage, $w = w_b$ [22, 23].

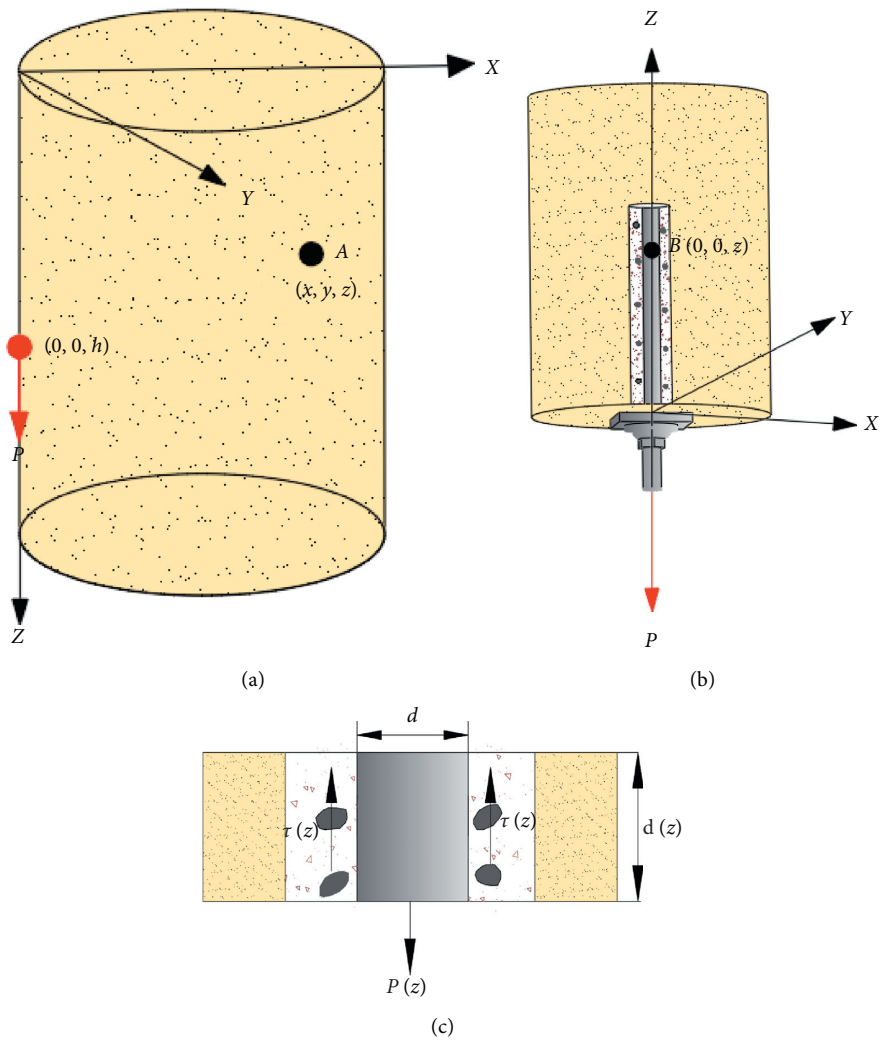

Figure 3: Mechanical model of bolt axial force distribution under the condition of resin grout with aggregate. (a) Calculation model of Mindlin displacement solution; (b) simplified calculation model; (c) diagram of microelement stress calculation.

$$\tau(z) = \frac{2\pi E}{(1+\mu)(3-2\mu)E_b A}\left(\int_0^z \tau(z)\mathrm{d}z\right)z. \tag{10}$$

Let $m = 2\pi E/((1+\mu)(3-2\mu)E_b A)$, and substituting it into equation (10) yields

$$\tau(z) = -m\left(\int_0^z \tau(z)\mathrm{d}z\right)z. \tag{11}$$

It can be derived that

$$\tau(z) = c\left(-\frac{mz}{2}\right)\exp\left(-\frac{m}{2}z^2\right). \tag{12}$$

Substituting equation (12) into equation (8) yields

$$P(z) = \frac{C}{2}\pi d\ \exp\left(-\frac{m}{2}z^2\right). \tag{13}$$

According to the boundary conditions, at the initial anchorage section end of the bolt $P(z)|_{z=0} = P$, the following results can be obtained:

$$C = \frac{2P}{\pi d}. \tag{14}$$

The distribution law of bolt shear stress along z direction is given by

$$\tau(z) = -\frac{mPz}{\pi d}\exp\left(-\frac{mz^2}{2}\right). \tag{15}$$

The distribution law of axial force of bolt along z direction is as follows:

$$P(z) = P\ \exp\left(-\frac{mz^2}{2}\right). \tag{16}$$

According to equation (14), the relationship among the shear distribution of bolt-resin interface, anchorage length, and E/E_b can be obtained as in Figure 4(a); the shear stress of bolt-grout interface, with the characteristics of large value and close to the initial anchorage section, produces a larger value at the initial anchorage section, then increases to the

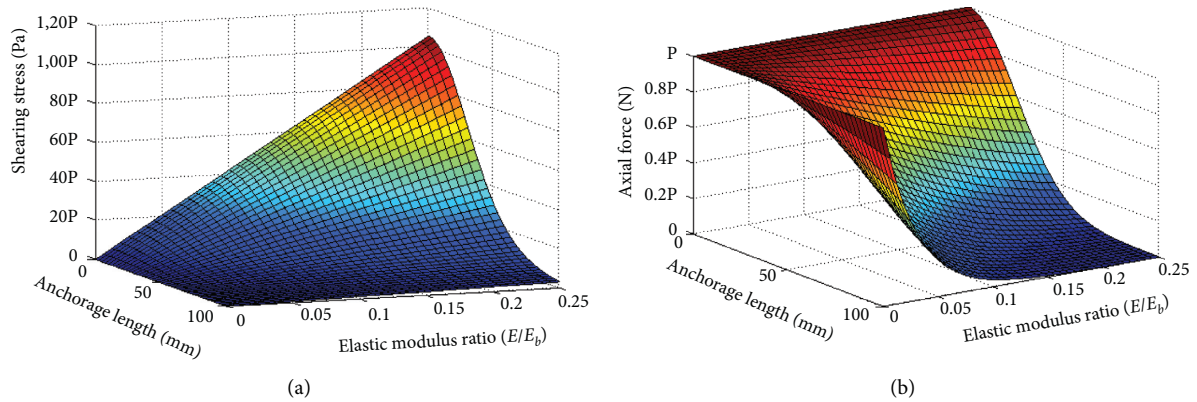

Figure 4: Distribution law of bolt-resin interface shear stress and bolt axial force. (a) Curved surface of bolt-resin interface shear stress; (b) curved surface of bolt axial force.

maximum value, and decreases sharply with the increase of anchorage length.

When the anchorage length increases to a certain extent, the end of the anchorage section almost does not produce shear stress. Moreover, the magnitude and distribution range of shear stress are also affected by the elastic modulus ratio E/E_b of resin grout and bolt. The greater the value of the ratio, the greater the value of the shear stress at the end of the anchorage section, and the larger the range of the shear stress distribution along the anchorage direction. Therefore, the shear stress of the bolt-resin interface provides a higher anchoring force.

According to equation (16), the relationship among axial force distribution of bolt, anchorage length, and E/E_b can be obtained as in Figure 44(b). It is clear that the axial force of the bolt is unevenly distributed. The bolt bears the maximum axial force at the initial anchorage section, which is equal to the pullout force or the load exerted by surrounding rock deformation. The mechanical properties of resin grout cannot change the axial force at the initial anchorage section, but the axial force distribution state of the bolt is significantly affected by the elastic modulus ratio E/E_b of resin grout and bolt. With the increase of E/E_b, the distribution range of bolt axial force decreases sharply. When the anchorage length increases to a certain extent, there is almost no axial force at the end of the bolt.

It can be concluded that the modification of resin grout mechanical properties can shorten the distribution range of axial force. The smaller the range of the axial force distribution, the higher the reliability of resin grout. To the bolt support of incompact fractured rock, strong disturbance rock, and deep roadway surrounding rock, the elastic modulus of resin grout increased, and the anchorage quality can be improved. It can be seen from equations (17) and (18) that the addition of metal aggregate in resin grout has a significant effect on the improvement of elastic modulus [24, 25].

The Voigt model considers that grout and aggregate bear the same stress, so the lower bound solution of elastic modulus is obtained as follows:

$$E = E_m V_m + E_f V_f. \tag{17}$$

The Reuss model considers that grout and aggregate bear the same strain, so the upper bound solution of elastic modulus is obtained as follows:

$$\frac{1}{E} = \left(\frac{V_m}{E_m} + \frac{V_f}{E_f}\right). \tag{18}$$

where E is the elastic modulus of resin grout with aggregate; E_m is the elastic modulus of pure resin grout; E_f is the elastic modulus of aggregate; V_m is the volume fraction of pure resin grout; and V_f is the volume fraction of aggregate.

Both the upper and lower limit values are higher than the elastic modulus of pure resin grout, and E increases with E_f. It can be concluded that the addition of metal aggregate in resin grout has a significant effect on the improvement of elastic modulus.

Adding steel segments with a certain length diameter ratio can not only significantly improve the elastic modulus of resin but also interact with the rib of the bolt; the improvement of the anchorage performance is more significant. Therefore, it is necessary to further study the addition of steel section in the resin to improve the bearing capacity of the anchorage system.

2.2. Analysis of Steel Segment Mechanical State. Two typical types of steel segment were used to explain the working mechanism in resin grout. The possible distribution of the two types of steel segment can be seen in Figure 5. Figures 5(a) and 5(b), respectively, represent the distribution state and working mechanism of two typical steel segments in resin grout. One side of the steel segment is the bolt, and the other side is the surrounding rock.

For the tenuous steel segments, as shown in Figure 5(a), after completing the mixing, the distribution patterns of tenuous steel segments can be summarized as follows: (a) the steel segments are horizontally distributed along the axial direction of the bolt; in the process of bolt pullout, the steel segments are mainly subjected to shear stress; (b) the steel segments are inclined and under tensile stress; and (c) the steel segments are approximately vertical, bearing compressive stress.

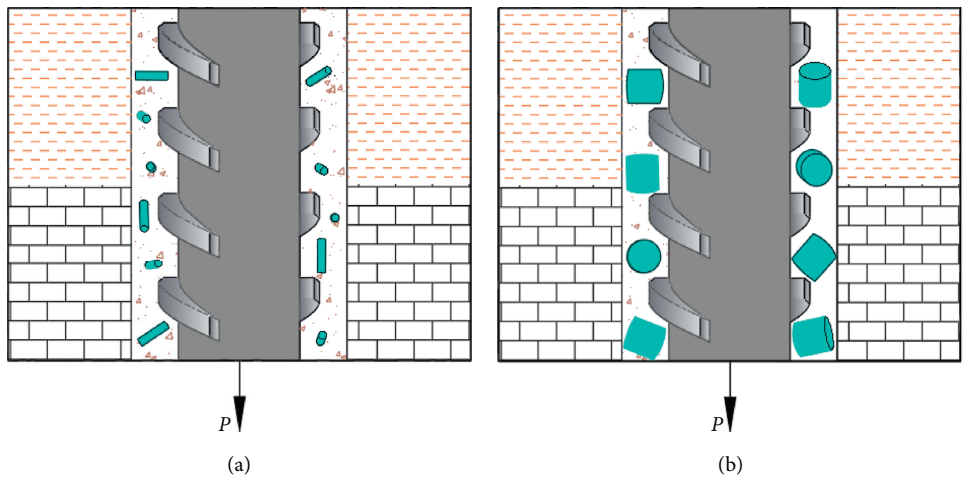

Figure 5: Distribution state and working mechanism of steel segments in resin grout. (a) Distribution state of the tenuous steel segment and working mechanism in resin grout; (b) distribution state of the coarse steel segment and working mechanism in resin grout.

For the coarse steel segments, as shown in Figure 5(b), the distribution patterns of coarse steel segments can be summarized as horizontally distributed, inclined distributed, and vertically distributed. Under those conditions, the steel segments bear the combined action of tension (compression) and shear stress.

As a brittle material, small deformation will lead to resin grout failure. Based on the relevant research conclusions, the elastic modulus, shear strength, and tensile strength of resin have a significant impact on the stability of the anchorage system [19, 26, 27]. However, the steel segment shows composite characteristics, rigid characteristics in the elastic stage, and ductile characteristics after yielding, so it has a high bearing capacity. The tensile strength, compressive strength, and shear strength of the steel segment are higher than those of resin grout.

3. Numerical Simulation of Bearing Capacity of Resin Grout with Steel Segment

Based on the aforementioned conclusions, the finite element numerical simulation software ABAQUS was used to further analyze the bearing performance of the pure resin with steel segments. The bearing capacity of resin grout without steel addition, 0.6 mm steel segment with 10 adding amount, and 3.0 mm steel segment with 10 adding amount were simulated, respectively.

3.1. Numerical Simulation Modeling. Modeling: 3D machinery software Solidworks was used to build a real form of a bolt, resin grout, steel sleeve, and steel segment, the bolt length was 200 mm with diameter 20 mm, and steel sleeve length was 100 mm with inner diameter 30 mm and outer diameter 45 mm. The method of Boolean operation was used to generate rib grooves in resin grout. To improve the solution accuracy and reduce calculation cost, the anchorage length with 5 mm annular thickness was determined to be 50 mm. After the completion of the model, it is saved as a sat format file, imported into ABAQUS software for meshing grids, giving material properties and imposing boundary conditions, and finally submitted for analysis and calculation [28, 29].

Meshing: combined with the parts shape and calculation cost, diversity grid types and sizes are selected for different regions. Tetrahedral element C3D10M was selected as the bolt and resin grout, hexahedral element C3D8I was selected for steel section, and hexahedral element C3D4 was selected for steel sleeve. The mesh size of the bolt and resin grout in the anchorage area was set to 2 mm and 3 mm in other areas of the bolt. The mesh size of 3 mm diameter steel segments was 0.3 mm, and that of 0.6 mm diameter steel segments was 0.08 mm. The number of mesh elements is shown in Table 1.

Boundary conditions and material parameters: the steel sleeve boundary was fixed to restrict its displacement and rotation. Using dynamic analysis, a constant loading speed of 1 mm/s was applied at the end of the bolt for pullout; the material property parameters of similar parts are the same in the simulation scheme. Bolt, steel segment, and steel sleeve were applied with elastic materials; resin grout was endowed with shear-damage failure criterion and plastic model, with C50 concrete material parameters as in [30].

The models and components are shown in Figure 6.

Material parameters are shown in Table 2. Bolt-grout and steel segment-grout interface were applied with contact properties; grout-steel sleeve interface was bound by "tie" contact.

3.2. Analysis of Bearing Characteristics of Resin Grout with Steel Segment. The mechanical properties of resin grout were improved by adding a steel segment. From the displacement contour map of three types of resin grout under the same axial stress (50 MPa) in Figure 7, it can be seen that the axial displacement of grout with steel additive is less than that of pure resin grout, and the axial displacement of grout with 3 mm diameter steel segment is less than that of the grout with 0.6 mm diameter steel segment. The simulation

Table 1: Number of mesh elements for different numerical models.

Parts	Numerical simulation scheme		
	Without addition	$D = 0.6$ mm; $L = 3$ mm	$D = 3$ mm; $L = 3$ mm
Bolt	16021	16021	16021
Resin grout	7893	7696	7256
Steel sleeve	4080	4080	4080
Steel segment	—	20790	31800

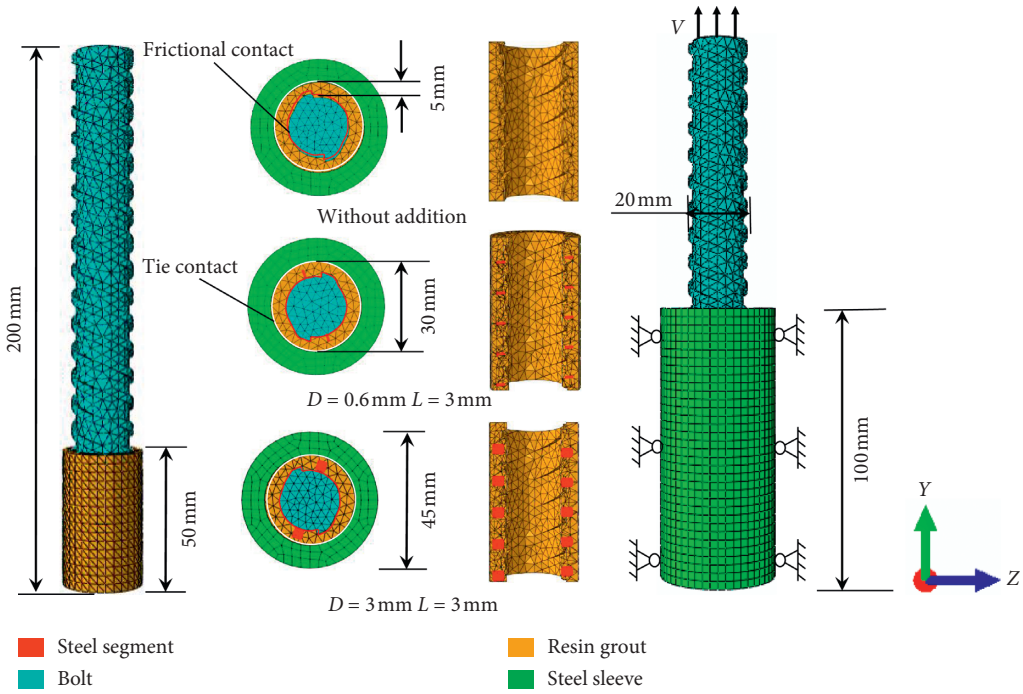

Figure 6: Numerical calculation model.

Table 2: Material parameters of the numerical calculation model.

Parts	Density (kg/m^3)	Elastic modulus (GPa)	Poisson ratio
Bolt	7800	208	0.25
Steel sleeve	7850	209	0.25
Steel segment	7800	205	0.26
Resin grout	2100	15	0.3

results show that the resin grout with steel segment has higher anchorage system stiffness and better load transfer capacity.

Figure 8 shows the displacement and stress contour map of different types of resin grout under peak stress. The peak stress and corresponding displacement of the resin grout with the addition of the steel segment are significantly increased, and the peak stress and corresponding displacement of resin grout with the 3 mm diameter steel segment are further improved compared with the 0.6 mm diameter steel segment. The simulation results show that the energy absorption capacity of the anchorage system with the steel segment is higher than that of pure resin, and the energy absorption capacity of the coarse steel segment is higher than that of the tenuous steel segment, which is more conducive to controlling the deformation of surrounding rock.

Figure 9 shows the stress and corresponding displacement contour map of three types of resin grout at the postpeak stage. It can be seen that when the grout is broken, the displacement of resin grout with 0.6 mm diameter steel segment is larger than that of the pure resin grout, and the bearing capacity of the postpeak stage also increased significantly; the bearing capacity of resin grout with 3 mm diameter steel segment has improved further. The simulation results show that the addition of steel segments in the resin grout can significantly improve the deformation resistance and failure resistance and thus improve the stability of the anchorage system.

Figure 10 shows the axial force-displacement curves of bolts with three types of resin grout. As can be seen from the figure, the load-displacement curve of pure resin grout is relatively smooth, and the axial force drops sharply at the postpeak stage. The slope of the axial force-displacement curve of resin grout with 0.6 mm diameter steel segment is greater than that of the pure resin grout at the elastic stage. When approaching the peak load of pure resin grout, the curve fluctuates and rises, and the peak load increases significantly. The falling slope after the peak load is smaller than

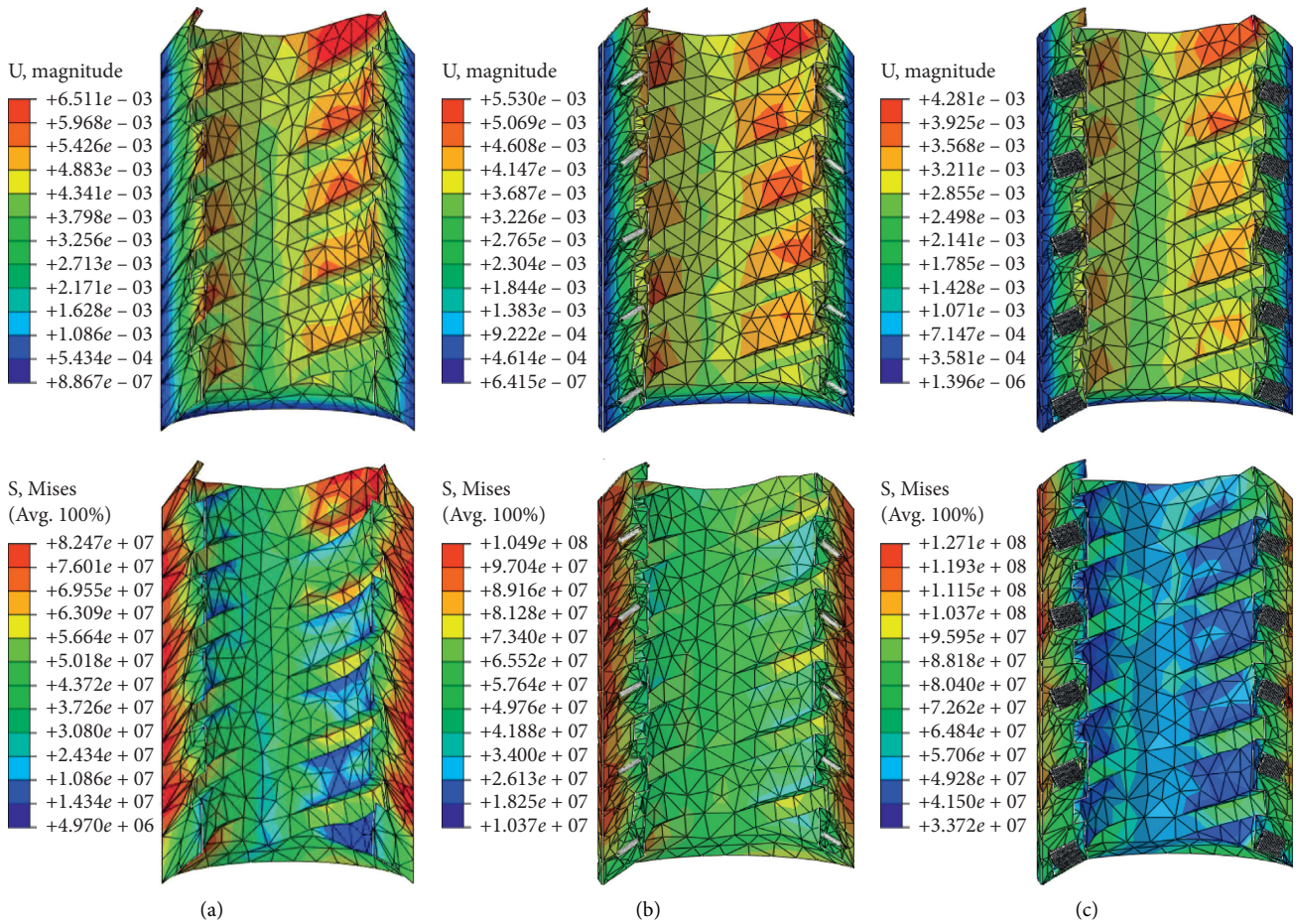

Figure 7: Displacement contour map of three types of resin grout under the same axial stress: (a) pure resin grout, (b) resin grout with 0.6 mm diameter steel segment, and (c) resin grout with 3 mm diameter steel segment.

that of the pure resin and still fluctuates, and the ultimate failure displacement is larger than that of the pure resin grout.

The bearing capacity of resin grout with the 3 mm diameter steel segment is the best among the three schemes, and the elastic stage slope of the axial force-displacement curve is the greatest. Similarly, the curve fluctuates when the load approaches the bearing capacity of pure resin grout, and the fluctuation amplitude further increases. The falling slope after the peak load is the smallest, and it shows obvious ductile deformation characteristics. The possible reason for the fluctuation of the load-displacement curve is that when the load is close to the bearing capacity of the pure resin agent, due to the large difference in the material properties of the resin grout and steel segment, the effect of the steel segment in the resin grout increases gradually and thus enters the load transfer and the coordinated deformation dynamic equilibrium process.

Stiffness and energy absorption capacity of the anchorage system are important indicators to evaluate anchorage quality [13, 19, 31]. The stiffness is the slope of the initial linear stage in the stress-displacement curve, and the energy absorption capacity is expressed by the area contained in the load-displacement curve from 0 to the peak load. Numerical simulation results of three different types of resin grout of the stiffness and energy absorption capacity are shown in Table 3.

The above data show that the addition of steel segment in the resin can improve the stiffness of the anchorage system. Under the condition of the same axial force generated by rock deformation, the axial displacement of resin grout with steel segment additive is less than that of pure resin grout, so the grout is easier to maintain integrity. At the same time, the absorption energy of resin grout with steel segment additive increases, and the ability to resist failure is enhanced. Under the dynamic and static load, the stability of the anchorage system can be further improved.

4. Bolting Performance Test for Steel Segment Additive Resin Grout

In order to further study the influence of length diameter ratio and adding amount of different steel segments on the anchorage performance, the anchoring force test was carried out in the laboratory to find the optimal adding amount and length diameter ratio.

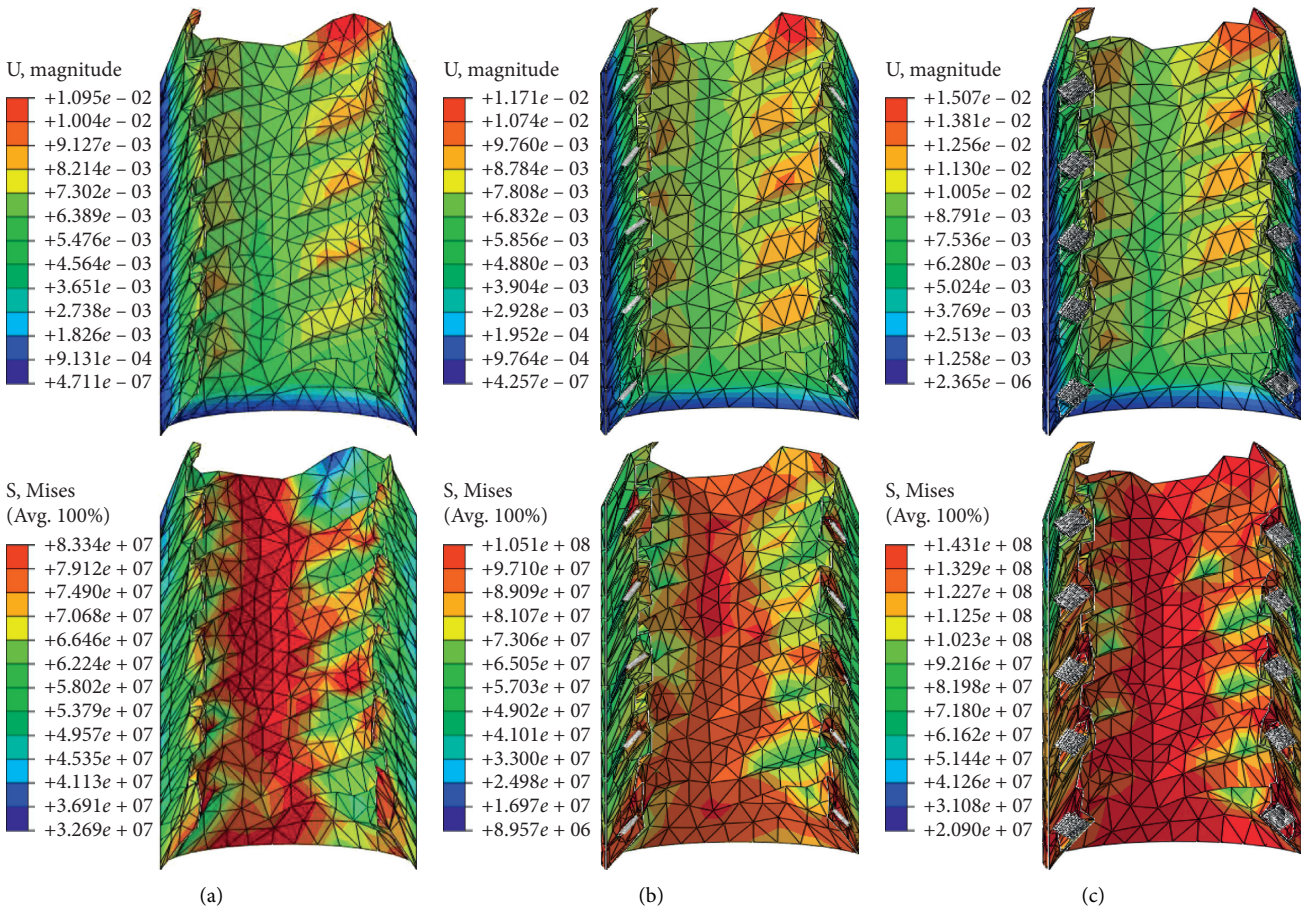

FIGURE 8: The peak stress and corresponding displacement of three types resin grout: (a) pure resin grout, (b) resin grout with 0.6 mm diameter steel segment, and (c) resin grout with 3 mm diameter steel segment.

4.1. Fabrication of Anchorage Specimens. The 20MnSi bolts used herein had left-hand threading, were 20 mm in diameter, and had 1.7 mm rib height, 13.7 mm rib spacing, 4.5 mm bottom rib width, and 3.3 mm top rib width (Figure 11(a)). A bulk medium-speed resin grout was used, whose gel time was 180 s, and curing time was about 10 min. Complying with the Chinese coal industry standard MT146.1-2011 [6], we used a mass ratio of catalyst to resin of 0.04 herein. The 90 g of resin needed for each experiment was weighed with a balance, and the 3 mL of catalyst needed was extracted with an industrial injector. The matching method of resin cement and curing agent used herein is shown in Figure 11.

The 3 mm length steel segment cut by fixed-length cutting machine was chosen to correspond to the annular thickness of resin grout; preliminary experimental results found that steel segments greater than 4 mm may cause drill sticking issues and thus greatly affect the mixing effect of resin induce low anchoring force values. The selection of steel segment used herein was 0.6, 1.2, 2.1, and 3.0 mm, whose tensile strength is 417.09 MPa~421.19 MPa and the elastic modulus is 174 GPa~199 GPa [32]. The steel segments were dosed into the grout resin by adding a varying number of segments into the 90 g of resin measured initially. These adding amounts were chosen as 20, 30, 40, 50, and 60 segments in the measured resin material, compared with the group without additive. There are a total of 21 groups for the test, with 3 specimens in each group, and a total of 63 test specimens. The experimental scheme is shown in Table 4.

Steel sleeves were used to simulate the bolt drilling and surrounding rock, featuring an inner diameter of 30 mm, a length of 100 mm, and a wall thickness of 7.5 mm (Figure 12(a)). To avoid slippage of anchoring agent in the inner wall of the sleeve during the pulling test, the entire length of the sleeve along the inner wall was threaded. The sides of the sleeve were smoothed for easy clamping and fixing (Figure 12(b)), and the end of the sleeve was simply welded. In this way, we ensured that the resin did not overflow and could be easily removed and ensured convenient observation of the bolt centering and the solidification of the resin grout (Figure 12(c)). A cap-shaped sealing device was designed to prevent ejection of resin grout during mixing and poorly centered of the bolt; the sealing device was printed using a 3D printer and featured a threaded body part whose outer diameter, threads, and pitches, respectively, matched the inner diameter, threads, and pitches of the sleeve (Figure 12(d)).

Based on the self-developed anchoring mixing device, the bolt is driven to mix the resin grout; the drilling rig rotation speed ranged from 0 to 1,000 r/min; the thrust range

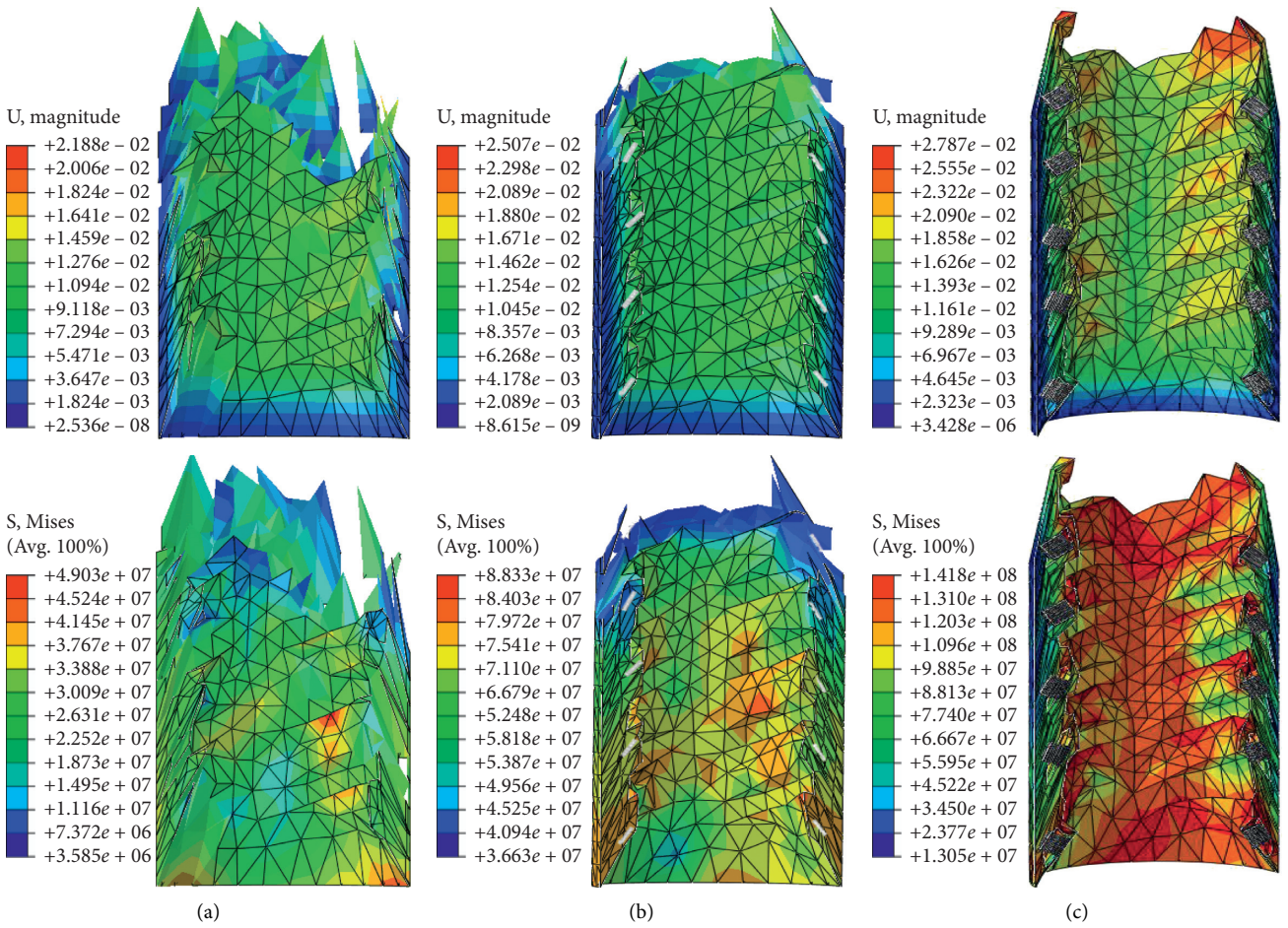

Figure 9: The stress and corresponding displacement of three types of resin grout at the postpeak stage: (a) pure resin grout, (b) resin grout with 0.6 mm diameter steel segment, and (c) resin grout with 3 mm diameter steel segment.

was 0–100 kN, and the adjustable range of stroke was 0–350 mm, as shown in Figure 13. This anchoring mixing equipment could thus simulate the working state of the bolt. During the experiment, the rotation speed was set to 500 r/min, the thrust was 50 kN, and the mixing time was 25 s.

After the resin grout was solidified, the specimen was removed from the anchoring mixing machine and placed in a curing box (SHBY-40B, Hebei Changji Instrument Co. Ltd., Cangzhou, China) with a 220 V rated power supply, 1,000 W operating power, and set temperature range of 10~200°C (Figure 14). According to the actual conditions of the project, the temperature was set at 15~20°C, and the relative humidity was set at 55%~60% with a curing time of 2 h [33, 34].

4.2. Anchorage Performance Test and Result Analysis

4.2.1. Pullout Test. A microcomputer-controlled electro-hydraulic servo universal testing machine (YNS-300, Sinotest Equipment Co. Ltd., Changchun, China) was used to test the anchoring force, whose maximum test force was 300 kN (Figure 15). The anchorage specimen was placed in the pullout test tool, whereupon the stress-displacement curves and data were obtained by setting the loading mode and the parameters.

The pullout test was carried out for the anchorage specimens with different types and by adding the amount of steel segment. The control unit was started; the pullout test tool and bolt were fixed with clamps. The loading mode was set as the displacement closed loop, with the speed of 2 mm/min; the load and displacement are collected by the inner load sensor and displacement sensor, respectively. After the peak load of the specimen decreased to a certain extent, the data acquisition was stopped [35]. The experimental phenomena were observed, and the load-displacement curve was recorded during the test.

As shown in Figure 16, all the failures occur along with the bolt-grout interface, the failure surface with additives is rougher than that without additives, as shown in Figures 16(a) and 16(b), and steel segment falls out continuously, as shown in Figures 16(c) and 16(d). It is observed that the peak load of the part specimens with additive increases, while that of other specimens with steel segment decreases. After the test completion, the bottom-end cover of the sleeve was opened. It can be observed that under the condition of a large amount of addition, part of the steel segments deposit at the bottom, which results in these

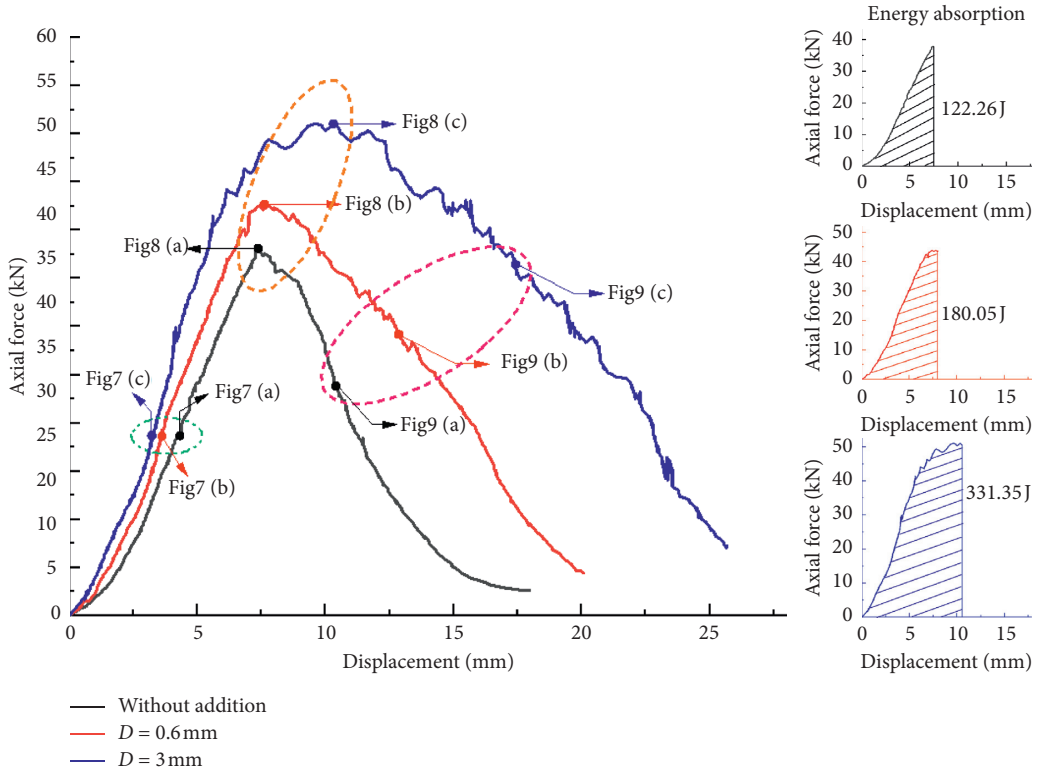

Figure 10: Axial force-displacement curves of different types of resin grout.

Table 3: The stiffness and energy absorption of different types of the anchorage systems.

Evaluation indicator	Addition type		
	Without	$D = 0.6$ mm; $L = 3$ mm	$D = 3$ mm; $L = 3$ mm
Stiffness (kN/mm)	6.05	7.03	7.47
Energy absorption (J)	122.26	180.05	331.35

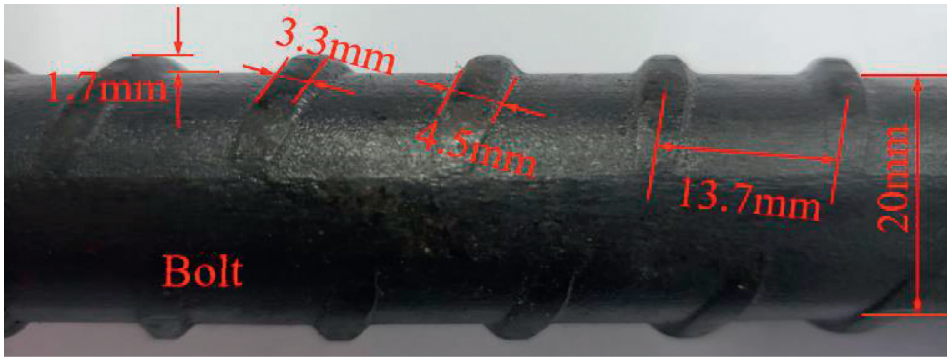

(a)

Figure 11: Continued.

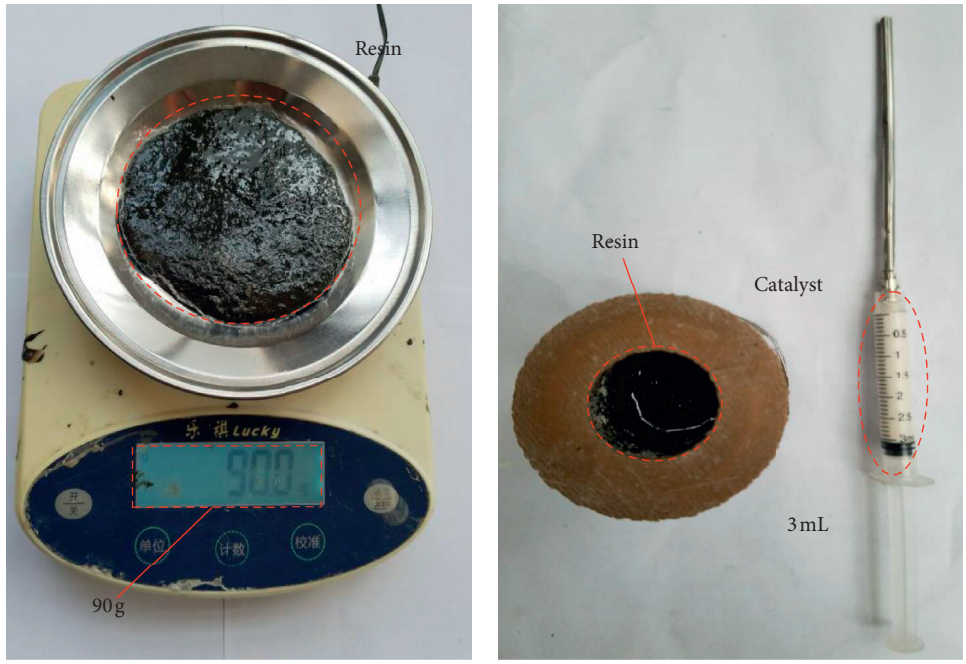

(b) (c)

Figure 11: Photographs demonstrating the bolt, quantitative method for resin, and catalyst measurement: (a) bolt for pullout tests, (b) weighing the resin with a balance, and (c) the mixedness of resin and catalyst.

Table 4: Experiment design for steel segment of varying diameter and adding amount.

No.	Length (mm)	Diameter (mm)	Adding amount (segment)	Remark
A	—	—	—	Without addition
B1	3.0	0.6	20	Φ 0.6 mm
B2	3.0	0.6	30	
B3	3.0	0.6	40	
B4	3.0	0.6	50	
B5	3.0	0.6	60	
C1	3.0	1.2	20	Φ 1.2 mm
C2	3.0	1.2	30	
C3	3.0	1.2	40	
C4	3.0	1.2	50	
C5	3.0	1.2	60	
D1	3.0	2.1	20	Φ 2.1 mm
D2	3.0	2.1	30	
D3	3.0	2.1	40	
D4	3.0	2.1	50	
D5	3.0	2.1	60	
E1	3.0	3.0	20	Φ 3.0 mm
E2	3.0	3.0	30	
E3	3.0	3.0	40	
E4	3.0	3.0	50	
E5	3.0	3.0	60	

sections do not form an anchoring effect with the bolt; after the bolt pulled out, the anchorage thin layer retained at the bottom of the sleeve, as shown in Figures 16(e) and 16(f).

4.2.2. Analysis of Anchorage Performance Test Results. The load-displacement curves of groups A–E are shown in Figure 17.

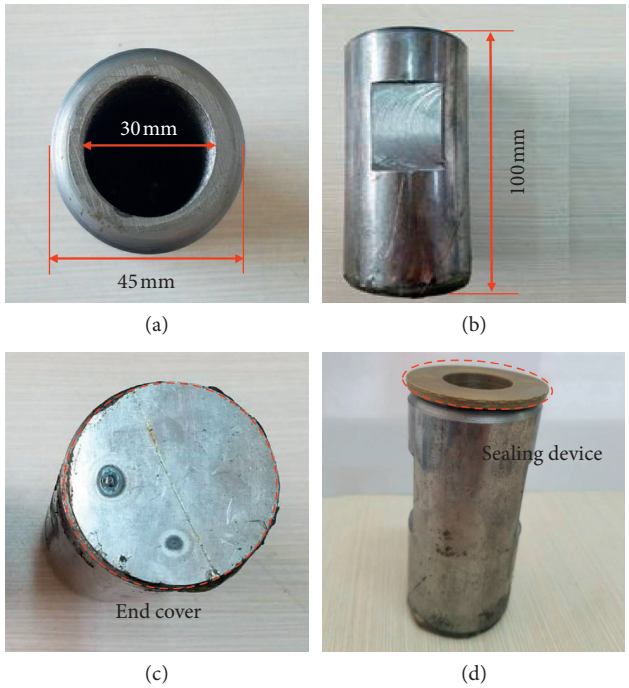

Figure 12: Photographs of the sleeve (steel tube) used in the experiment, showing the sleeve in (a) top view, (b) side view, and (c) bottom view; (d) after assembly of the sealing device.

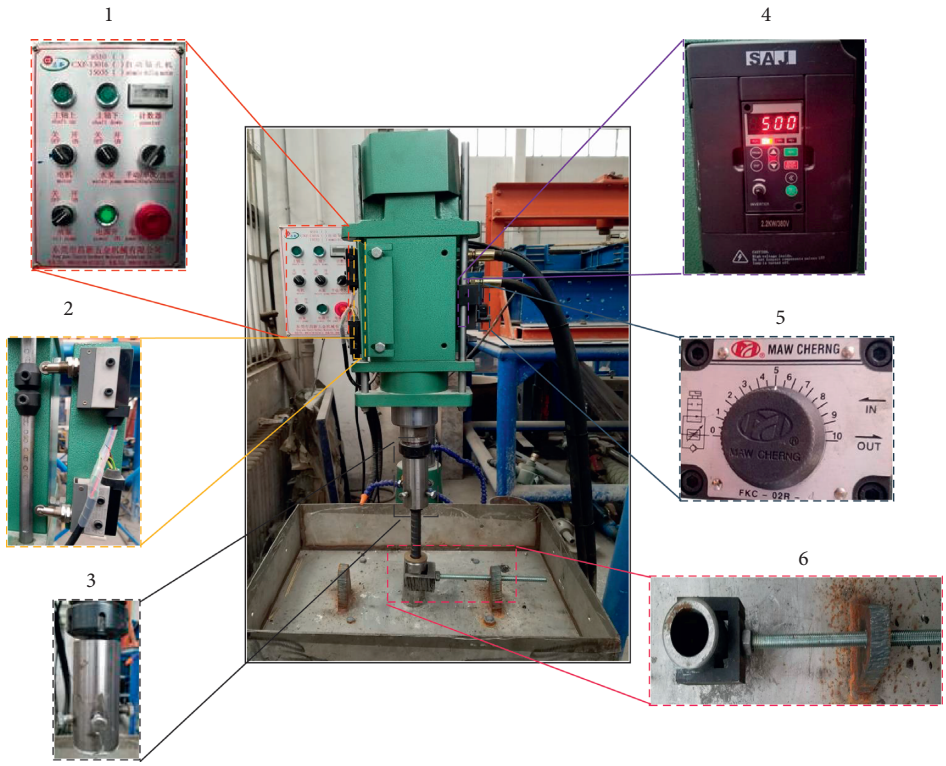

Figure 13: Photographs of the mixing and anchorage equipment, showing details of the (1) operation control panel, (2) distance sensor, (3) chuck conversion device, (4) speed control panel, (5) thrust control knob, and (6) sleeve fixing device.

From the load-displacement curves of each group, it can be seen that the load-displacement curves of resin grout with different types of steel segments are significantly different from those of pure resin grout. Within a certain range, the peak loads increase rapidly with the increase of the number of steel segments, and the corresponding displacements of

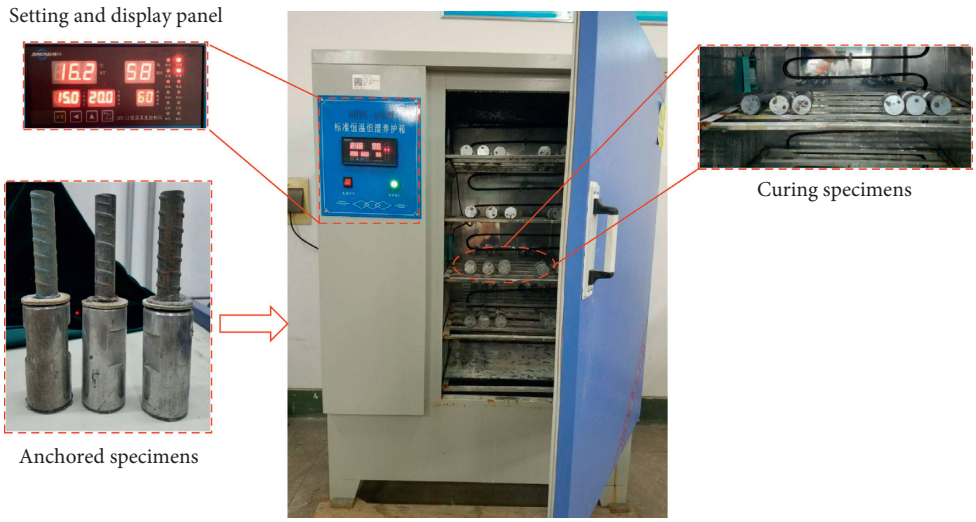

Figure 14: Photographs of equipment used for curing the anchorage specimens, showing details of the setting and display panel (upper left), anchored specimens (lower left), and curing specimens (upper right).

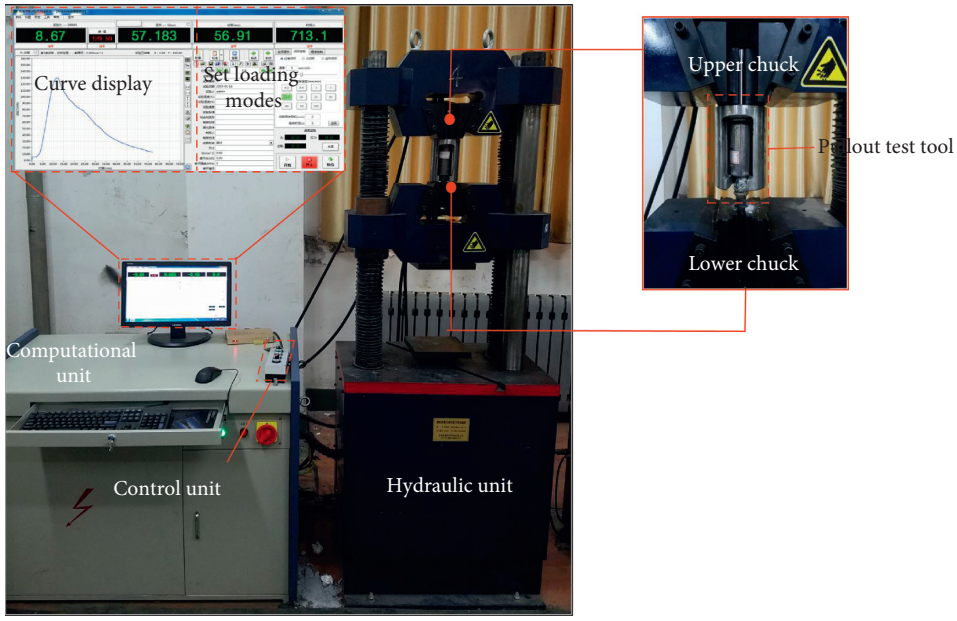

Figure 15: Photographs of the pullout test equipment, showing details of the computational unit with a data display and set loading modes (upper left) and the upper and lower chucks flanking the pullout test tool (upper right).

the peak load (hereafter referred to as the peak displacements) are different, and the peak displacements of pure resin grout in group A is within the range of 9.7–10.1 mm. The peak displacement of group B increased from 10.5 mm (20 segments) to 11.9 mm (40 segments). With the adding amount further increased, the peak displacement decreases. The peak load and peak displacement of each specimen in the same group show a large discrete degree. The peak displacement of group C increased gradually within the adding amount of 20–50 segments. When the adding amount reaches 60 segments, the peak load and peak displacement discrete degrees increase, but the discrete amplitude was significantly lower than that of group B under the same adding amount; the peak displacement of group C ranged from 8.2 mm to 12.1 mm. The peak displacement of group D is within the range of 10.1–12.5 mm, and that of group E is 9.8–13.5 mm. In groups D and E, the peak displacement of 20–40 segments additive increases gradually and decreases significantly with the further increase of adding amount, but the discrete amplitude of peak load and peak displacement in the same group is small. The peak load and peak displacement of groups D and E reach the maximum when the adding amount is 40 segments, and the load-displacement curve shows ductile deformation characteristics [36].

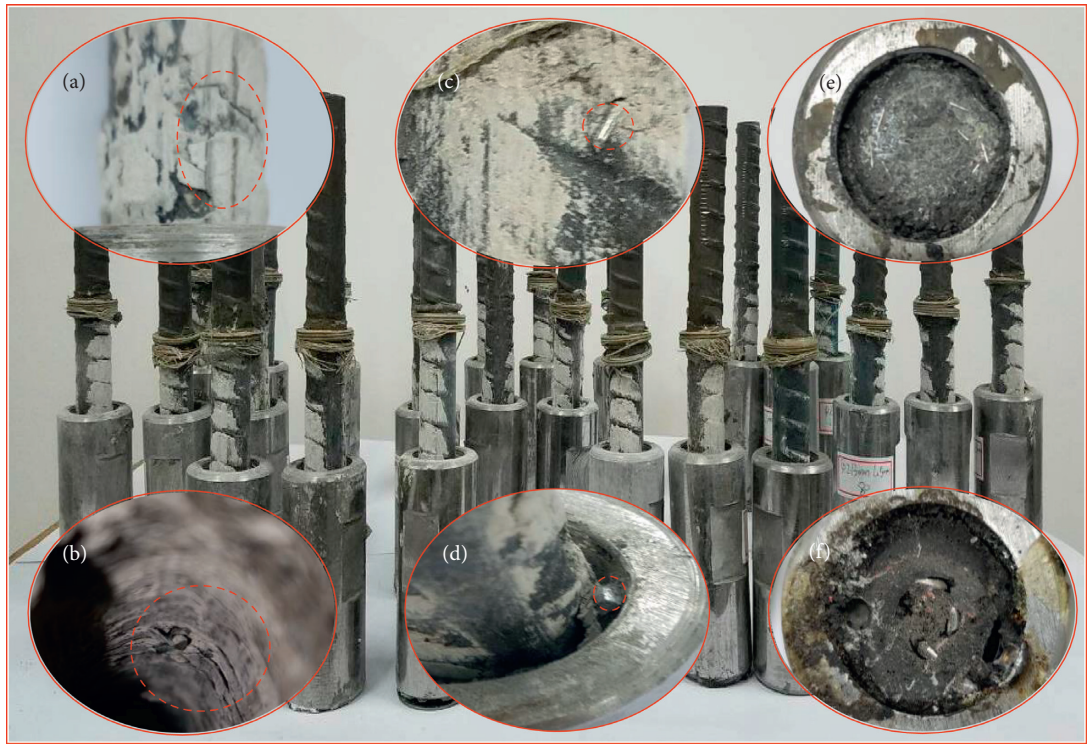

Figure 16: Photographs of portions of the specimens after completion of the pullout test and experimental phenomena: (a and b) the rougher bolt-grout interface of specimens with additives, (c and d) steel segment distribution state, and (e and f) residual anchorage thin layer at bottom with a larger number of steel segments adding amount.

The average peak load and energy absorption capacity of each group are shown in Table 5. Table 5 is the average anchoring force and energy absorption capacity of each group. The above data show that the average anchoring force and energy absorption capacity of resin grout with additives are significantly different from those of pure resin grout. After adding a reasonable type and quantity of steel segments into resin grout, the anchoring force and energy absorption capacity of the bolting system can be significantly improved, which is more conducive to the control of rock deformation. The following rules can be obtained by analyzing the data in Table 5.

(a) The bearing capacity and energy absorption of the anchorage system are significantly improved by adding a certain amount of steel segments into the resin grout. For four types of steel segments with 0.6 mm, 1.2 mm, 2.1 mm, and 3.0 mm, the average peak load and energy absorption of each group is higher than that of pure resin within the range of 50 segments, which further verifies the conclusion of numerical simulation.

(b) The improved efficiency of different steel segment types on anchorage performance is different. Taking 40 segments of four types of steel segments as an example, the average peak pullout forces of each group are 114.56 kN, 126.88 kN, 141.53 kN, and 156.32 kN, respectively, which are 10.90%, 22.83%, 37.00%, and 51.33% higher than that of pure resin grout, and the energy absorption capacities are 599.09 J, 732.33 J, 788.61 J, and 1026.88 J respectively. Compared with the energy absorption capacity of pure resin grout, it is increased by 23.10%, 50.48%, 62.05%, and 111.01%, respectively. The larger the diameter of the steel segment, the better the anchorage performance.

(c) With the increase of steel segment addition, the bearing capacity of the anchorage system increases, and it decreases sharply when it reaches a certain value. When the steel segment addition exceeds a certain value, the anchoring force is even lower than that of the grout without steel segment addition. The possible reasons are as follows: (1) at the bolt-grout interface, a large amount of steel segments reduces the bolt anchorage range, which limits the bearing capacity of the anchorage structure; (2) under the condition of a large amount of steel segment addition, part of the steel segments deposited at the bottom during the mixing process, as shown in Figures 16(e) and 16(f), resulting in that the bolt cannot penetrate to the end, and the thin layer formed by the anchoring agent at the end does not form an anchoring effect with the bolt. Combined with Figure 18 for analysis, different types of steel segments have different improvements on the bearing capacity, and the optimal addition amount is different. The optimal adding amount of 0.6 mm diameter steel segment is 50, and that of steel segments with 1.2 mm diameter is 50 segments, that of

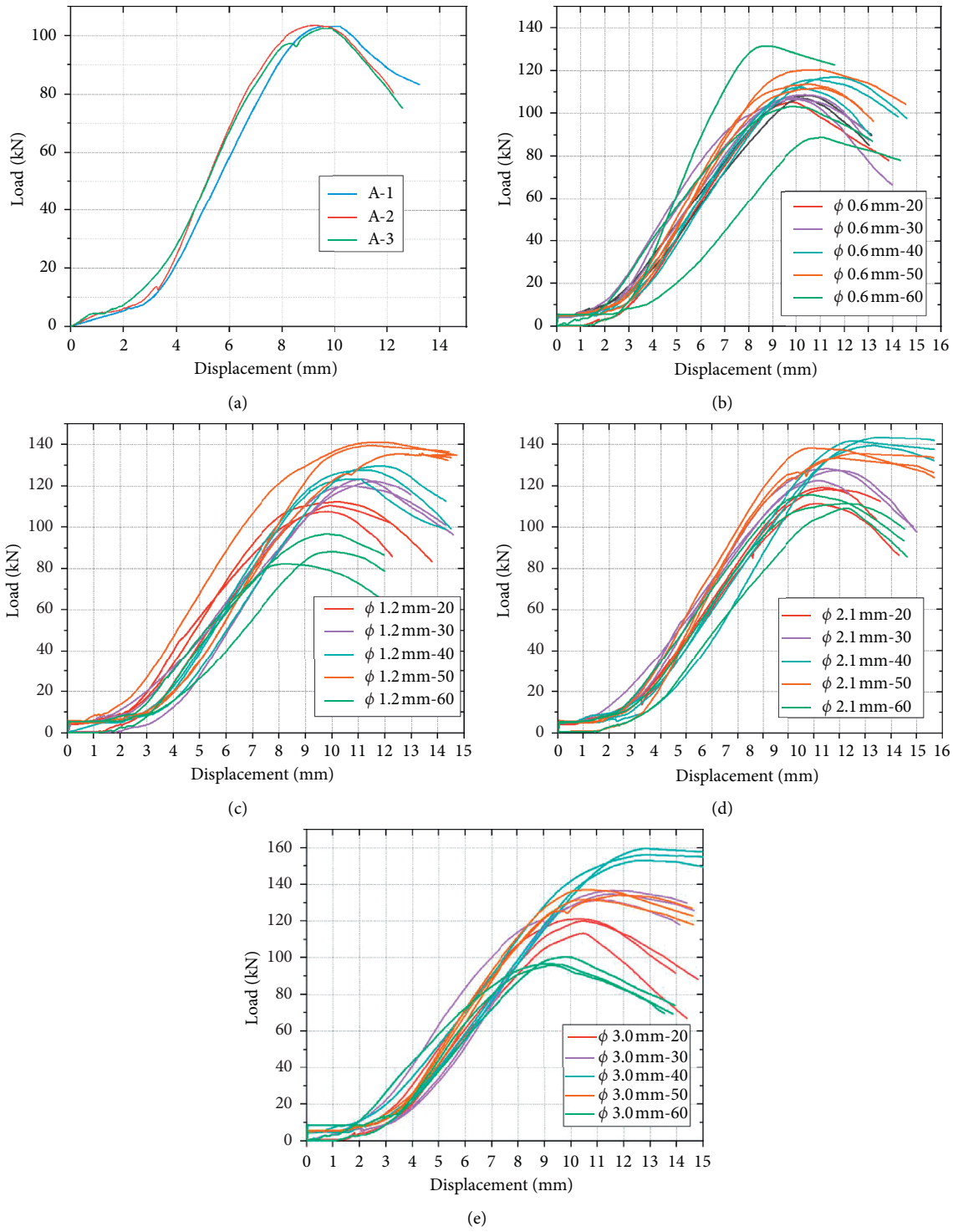

Figure 17: Load-displacement curves for each specimen from which data were measured for groups A–E: (a) load-displacement curves of pure resin grout, (b) load-displacement curves from group B; (c) load-displacement curves from group C; (d) load-displacement curves from group D; (e) load-displacement curves from group E.

Table 5: Average peak load and energy absorption capacity of each group.

Adding amount	Addition type							
	0.6 mm		1.2 mm		2.1 mm		3.0 mm	
	Peak load (kN)	Energy absorption (J)	Peak load (kN)	Energy absorption (J)	Peak load (kN)	Energy absorption (J)	Peak load (kN)	Energy absorption (J)
0	103.3	486.65	103.3	486.65	103.3	486.65	103.3	486.65
20	106.8	532.92	110.1	580.15	116.16	609.19	118.23	590.11
30	107.4	574.66	121.78	754.74	126.1	740.25	134.0	764.06
40	114.56	599.09	126.88	732.33	141.53	788.61	156.32	1,026.88
50	115.2	618.66	138.72	769.46	135.79	760.02	134.33	826.55
60	111.7	566.74	87.25	371.34	111.96	676.76	97.7	448.41

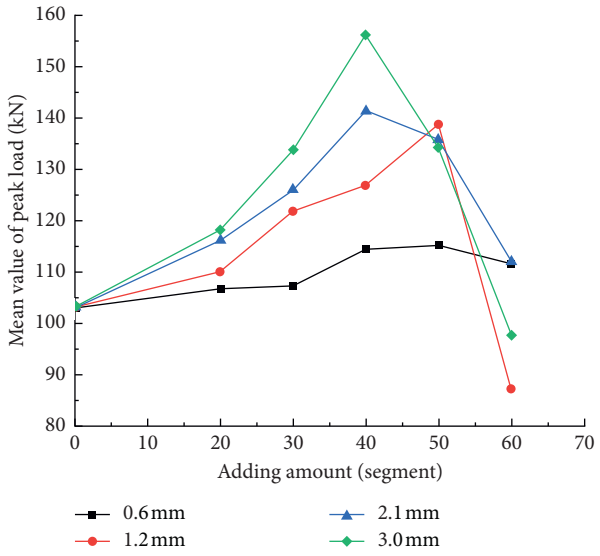

Figure 18: Effect of steel segment types and dosage on anchoring force.

steel segments with 2.1 mm diameter is 40 segments, and that of steel segments with 3.0 mm diameter is 40 segments.

Compared with the peak anchoring force of pure resin grout (103.3 kN), the peak load of resin grout with 0.6 mm, 1.2 mm, 2.1 mm, and 3.0 mm diameter steel segments under their optimal dosage conditions increased by 11.52%, 34.29%, 37.01%, and 51.3%, respectively. Therefore, the suitable type and adding the amount of steel segments into resin grout forms a composite resin that can significantly improve the bearing capacity and load transfer performance of bolting.

5. Conclusions

(1) The working mechanism of the steel segment in resin grout and its effect on anchorage performance was revealed by establishing mechanical model calculation and theoretical analysis. The calculation results of the mechanical model show that the addition of aggregate in the resin grout can improve the load transfer of the bolt. Based on this, it is proposed that the addition of steel segments can not only significantly improve the mechanical parameters of resin grout but also interact with the rib of the bolt, which has a more significant effect on the improvement of the anchorage performance.

(2) Using the finite element numerical simulation software ABAQUS, we presented an novelty numerical modeling that could be applied for evaluating bolting performance, the displacements, and axial load, and stress distribution state could be obtained. The numerical simulation results show that the stiffness and energy absorption capacity of the anchorage agent are improved by the incorporation of the steel segment, and the stiffness and energy absorption capacity of resin grout with coarse steel segment are higher than that of the tenuous steel segment. The load-displacement curves of the grout material after adding the steel segment present a transition from brittleness to ductility.

(3) Based on the self-developed anchorage mixing device, the experimental program was reasonably designed. The effect of different steel segment types and adding amounting on the anchoring force was tested, and the optimal dosage of different steel segment forms was obtained: the optimal adding amount of 0.6 mm diameter steel segment is 50, that of steel segments with 1.2 mm diameter is 50 segments, that of steel segments with 2.1 mm diameter is 40 segments, and that of steel segments with 3.0 mm diameter is 40 segments. Generally speaking, when the length of anchorage section is 10 cm, adding 40 steel segments with 3.0 mm diameter and 3.0 mm length can improve the anchorage performance most significantly.

Data Availability

The data used to support the findings of this study are included within the article.

Conflicts of Interest

The author declares no conflicts of interest.

References

[1] C. R. Windsor, "Rock reinforcement systems," *International Journal of Rock Mechanics and Mining Sciences*, vol. 34, no. 6, pp. 919–951, 1997.

[2] B. M. Laura, T. J. Michel, H. H. Faouzi, and N. Aurélien, "Assessment of the bolt-grout interface behaviour of fully grouted rockbolts from laboratory experiments under axial loads," *International Journal of Rock Mechanics and Mining Sciences*, vol. 63, pp. 50–61, 2013.

[3] J. Nemcik, S. Ma, N. Aziz, T. Ren, and X. Geng, "Numerical modelling of failure propagation in fully grouted rock bolts subjected to tensile load," *International Journal of Rock Mechanics and Mining Sciences*, vol. 71, pp. 293–300, 2014.

[4] E. Hoek and D. F. Wood, "Rock support," *International Journal of Rock Mechanics and Mining Sciences & Geomechanics Abstracts*, vol. 26, pp. 282–287, 1989.

[5] M. Ghadimi, K. Shahriar, and H. Jalalifar, "A new analytical solution for the displacement of fully grouted rock bolt in rock joints and experimental and numerical verifications," *Tunnelling and Underground Space Technology*, vol. 50, pp. 143–151, 2015.

[6] Q. L. Ding, J. M. Guo, Y. Zhang, and X. L. Wang, *China Coal Industry Standards-Part 1, MT/T 146.1-2011*, State Administration of Safety Production Supervision and Administration of China, Beijing, China, 2011.

[7] B. Hu, H. P. Kang, J. Lin, J. F. Cai, and P. F. Jiang, "Study on influence of temperature on anchorage performance of resin anchored bolt," *Journal of Mining & Safety Engineering*, vol. 29, pp. 644–649, 2012.

[8] N. Aziz, P. Craig, A. Mirzaghorbanali, and J. Nemcik, "Factors influencing the quality of encapsulation in rock bolting," *Rock Mechanics and Rock Engineering*, vol. 49, no. 8, pp. 3189–3203, 2016.

[9] K. Skrzypkowski, W. Korzeniowski, K. Zagórski, and A. Zagórska, "Flexibility and load-bearing capacity of roof bolting as functions of mounting depth and hole diameter," *Energies*, vol. 12, no. 19, p. 3754, 2019.

[10] S. Zhang, P. F. Gou, and H. Fan, "Influence of water and temperature on resin anchor-hold," *Journal of Southeast University: Natural Science Edition*, vol. 35, no. I, pp. 57–62, 2005.

[11] F. L. He, H. Yan, L. G. Yang, H. Z. Yang, and Q. Li, "Anchorage experimental research on a coal roadway with water spraying and broken roof and its application," *Rock and Soil Mechanics*, vol. 32, pp. 2591–2595, 2011.

[12] H. P. Kang, Q. L. Cui, B. Hu, and Z. G. Wu, "Analysis on anchorage performances and affecting factors of resin bolts," *Journal of China Coal Society*, vol. 39, pp. 1–10, 2014.

[13] K. Skrzypkowski, W. Korzeniowski, K. Zagórski, and A. Zagórska, "Modified rock bolt support for mining method with controlled roof bending," *Energies*, vol. 13, no. 8, pp. 1–20, 2020.

[14] A. S. Alqarni, A. S. Albidah, A. M. Alaskar, and A. A. Abadel, "The effect of coarse aggregate characteristics on the shear behavior of reinforced concrete slender beams," *Construction and Building Materials*, vol. 264, Article ID 120189, 2020.

[15] J. Huang, Z. Luo, and M. B. E. Khan, "Impact of aggregate type and size and mineral admixtures on the properties of pervious concrete: an experimental investigation," *Construction and Building Materials*, vol. 265, Article ID 120759, 2020.

[16] Y. Geng, M. Zhao, H. Yang, and Y. Wang, "Creep model of concrete with recycled coarse and fine aggregates that accounts for creep development trend difference between recycled and natural aggregate concrete," *Cement and Concrete Composites*, vol. 103, pp. 303–317, 2019.

[17] C. A You and Y. B. Zhan, "Analysis of interfacial slip mesomechanics in anchorage section of prestressed anchor cable," *Chinese Journal of Rock Mechanics and Engineering*, vol. 28, no. 10, pp. 1976–1985, 2009.

[18] C. Cao, T. Ren, and C. Chris, "Introducing aggregate into grouting material and its influence on load transfer of the rock bolting system," *International Journal of Mining Science and Technology*, vol. 24, no. 3, pp. 325–328, 2014.

[19] C. Cao, T. Ren, Y. Zhang, L. Zhang, and F. Wang, "Experimental investigation of the effect of grout with additive in improving ground support," *International Journal of Rock Mechanics and Mining Sciences*, vol. 85, pp. 52–59, 2016.

[20] M. Zhang, C. Cao, and H. D. Zhang, "Effect of anchoring force by adding steel aggregate in resin anchoring agent," *Journal of China Coal Society*, vol. 44, pp. 1690–1697, 2019.

[21] X. N. Gong, *Soil Mechanics*, China Building Industry Press, Beijing, China, 2002.

[22] H. X. Dong, J. Q. Fan, R. Li, J. Zhao, and H. L. Zhang, "Shear stress analysis of anchorage section of full length bonded bolt based on Mindlin displacement solution," *Protective Engineering*, vol. 34, pp. 29–33, 2012.

[23] C. A. You, "Stress analysis of full-length bonded bolt," *Chinese Journal of Rock Mechanics and Engineering*, vol. 19, pp. 339–341, 2000.

[24] Y. C. Chang, Y. Geng, Y. Y. Wang, and Q. H. Wang, "Models of elastic modulus for concrete made with recycled coarse aggregate based on two-phase composite material," *Journal of Building Structures*, vol. 41, pp. 165–173, 2020.

[25] F. P. Zhou, F. D. Lydon, and B. I. G. Barr, "Effect of coarse aggregate on elastic modulus and compressive strength of high performance concrete," *Cement and Concrete Research*, vol. 25, no. 1, pp. 177–186, 1995.

[26] A. Kilic, E. Yasar, and A. G. Celik, "Effect of grout properties on the pull-out load capacity of fully grouted rock bolt," *Tunnelling and Underground Space Technology*, vol. 17, pp. 355–362, 2002.

[27] S. C. Gu, G. F. Ye, and X. Chen, "Experiment on limit shearing strength parameters of bolt anchored section," *Coal Science and Technology*, vol. 38, pp. 37–40, 2010.

[28] Dassault Systemes SIMULIA Corp, *ABAQUS Analysis User's Manual Version 6.14*, DS Simulia Corp, Providence, Rhode Island, USA, 2014.

[29] Y. P. Shi and Y. R. Zhou, *ABAQUS Finite Element Analysis and Example Explanation*, China Machine Press, Beijing, China, 2006.

[30] N. Aziz, J. Hillyer, D. Joyce, S. Q. Ma, J. Nemcik, and A. Moslemi, "New approach to resin sample preparation for strength testing," in *Proceedings of the 13th Coal Operators' Conference*University of Wollongong, The Australasian Institute of Mining and Metallurgy & Mine Managers Association of Australia, Wollongnog, Austraila, 2013.

[31] S. Q. Ma, N. Aziz, J. Nemcik, and A. Mirzaghorbanali, "The effects of installation procedure on bond characteristics of fully grouted rock bolts," *Geotechnical Testing Journal*, vol. 40, pp. 846–857, 2017.

[32] M. M. Zhang, *Study on the Similarity Laws in Structural Model Testing Accounting For Nonlinear Performance of Structures*, M.S. thesis, Tianjin University, Tianjin, China, 2018.

[33] H. L. Hartman, J. M. Mutmansky, R. V. Ramani, and Y. J. Wang, *Mine Ventilation and Air Conditioning*, John Wiley & Sons, New York, NY, USA, 2012.

[34] C. Wu, *Mine Ventilation and Air Conditioning*, Central South University Press, Changsha, China, 3rd edition, 2008.
[35] T. Isabelle, B. M. Laura, H. H. Faouzi, S. Acques, L. Zbigniew, and W. Aleksander, "Laboratory pull-out tests on fully grouted rock bolts and cable bolts: results and lessons learned," *Journal of Rock Mechanics and Geotechnical Engineering*, vol. 9, pp. 843–855, 2017.
[36] M. F. Cai, M. C. He, and D. Y. Liu, *Rock Mechanics and Engineering*, pp. 843–855, The Science Publishing Company, Beijing, China, 2013.